

Journal of Bioactive and Compatible Polymers

<http://jbc.sagepub.com/>

Dose-dependent enhancement of bone marrow stromal cells adhesion, spreading and osteogenic differentiation on atmospheric plasma-treated poly(l-lactic acid) nanofibers

Wentao Liu, Qing Cai, Feng Zhang, Yan Wei, Xuehui Zhang, Ying Wang, Xuming Deng and Xuliang Deng

Journal of Bioactive and Compatible Polymers 2013 28: 453 originally published online 30 July 2013

DOI: 10.1177/0883911513494623

The online version of this article can be found at:

<http://jbc.sagepub.com/content/28/5/453>

Published by:



<http://www.sagepublications.com>

Additional services and information for *Journal of Bioactive and Compatible Polymers* can be found at:

Email Alerts: <http://jbc.sagepub.com/cgi/alerts>

Subscriptions: <http://jbc.sagepub.com/subscriptions>

Reprints: <http://www.sagepub.com/journalsReprints.nav>

Permissions: <http://www.sagepub.com/journalsPermissions.nav>

Citations: <http://jbc.sagepub.com/content/28/5/453.refs.html>

>> [Version of Record](#) - Sep 13, 2013

[OnlineFirst Version of Record](#) - Jul 30, 2013

[What is This?](#)

Dose-dependent enhancement of bone marrow stromal cells adhesion, spreading and osteogenic differentiation on atmospheric plasma-treated poly(L-lactic acid) nanofibers

Journal of Bioactive and
Compatible Polymers

28(5) 453–467

© The Author(s) 2013

Reprints and permissions:

sagepub.co.uk/journalsPermissions.nav

DOI: 10.1177/0883911513494623

jbc.sagepub.com



Wentao Liu^{1,2}, Qing Cai³, Feng Zhang⁴, Yan Wei¹, Xuehui Zhang⁵, Ying Wang¹, Xuming Deng² and Xuliang Deng¹

Abstract

Although poly(L-lactic acid) nanofibers are known to promote osteogenic differentiation of bone marrow stromal cells, their relative hydrophobicity and surface inertia tend to hinder their biomedical application. We explored a feasible and effective technique to improve the bioactivity and biocompatibility of poly(L-lactic acid) fibers for further application in regenerative medicine. A low-temperature atmospheric plasma was used to treat poly(L-lactic acid) nanofibers for 1, 5, and 10 min, and the surface properties and dose-dependent effects on the behavior of bone marrow stromal cells were studied. Both the amino group content and surface hydrophilicity of the nanofibers increased with treatment time, whereas the spreading and proliferation of bone marrow stromal cells were greatest on nanofibers which had been treated for 5 min, followed by samples treated for 1 and 10 min. The quantitative reverse transcription–polymerase chain reaction analysis of the bone marrow stromal cells on the 5-min-treated nanofibers had the highest expression level of osteogenic marker genes including RUNX2, BMP2, ALP, COL1A1, OPN, and OCN. The nanofibers treated for 5 min also promoted the high levels of alkaline phosphatase

¹Department of Geriatric Dentistry, Peking University School and Hospital of Stomatology, Beijing, P.R. China

²College of Veterinary Medicine, Jilin University, Changchun, P.R. China

³Key Laboratory of Carbon Fiber and Functional Polymers, Ministry of Education, Beijing University of Chemical Technology, Beijing, P.R. China

⁴The Oral Clinic of the 2nd Hospital of Beijing Armed Police Force, Beijing, P.R. China

⁵Department of Materials Science and Engineering, Tsinghua University, Beijing, P.R. China

Corresponding author:

Xuliang Deng, Department of Geriatric Dentistry, Peking University School and Hospital of Stomatology, Beijing 100081, P.R. China.

Email: kqdengxuliang@bjmu.edu.cn

activity. These results suggest the exertion of dose-dependent effects by atmospheric plasma treatment on the surface of poly(L-lactic acid) nanofibers, and that this treatment is a feasible and effective technique to improve biomaterial biocompatibility and promotion of osteogenic differentiation of bone marrow stromal cells.

Keywords

Biocompatibility, osteogenic differentiation, surface modification, poly(L-lactic acid) nanofibers, plasma treatment

Introduction

The current challenge in bone tissue engineering is to fabricate effective artificial bone grafts for the regeneration of fractured or diseased bones. Biomaterial surface properties have been reported to play a pivotal role in the regulation of cell behavior and the subsequent determination of their value in this application.^{1,2} The chemical, mechanical, and architectural cues of biomaterials can lead to specific cell responses and direct the osteogenic differentiation of mesenchymal stem cells (MSCs).^{3–6}

Electrospun nanofibrous membranes are considered to have great potential in the field of tissue engineering since they can closely mimic the extracellular matrix architecture.^{7–11} A number of reports have shown that scaffolds with randomly oriented nanofibers had proven favorable for the osteogenesis of bone marrow stromal cells (BMSCs) and stimulated bone formation.^{12,13} Previously, we had used poly(L-lactic acid) (PLLA) nanofibers to study the effects of fiber orientation on osteoblast-like MG63 cells morphology, proliferation, and differentiation.¹⁴ Random nanofibers led to increase of alkaline phosphatase (ALP) activity, as well as collagen IA1 (COL1A1) and osteocalcin (OCN) production, compared to tissue culture polystyrene (TCP). These results suggested that PLLA nanofiber scaffolds were promising biomaterials for facilitating osteogenesis. However, the relative hydrophobicity and surface inertia of PLLA electrospun nanofibers might be unfavorable for cell adhesion and spreading, and therefore hinder their further application.¹⁵

Low-temperature plasma treatment has been shown to be a convenient and effective way to modify surfaces to improve the hydrophilicity of biomaterials, and so increasing biocompatibility and facilitating cell attachment.^{16,17} Wan et al.¹⁵ reported that ammonia plasma treatment significantly increased the hydrophilicity of poly(lactic acid) (PLA) scaffolds and resulted in enhancement of cell adhesion and proliferation of mouse 3T3 fibroblasts. D'Sa et al.¹⁸ reported that improved hydrophilicity of poly(methyl methacrylate) (PMMA) surfaces by plasma treatment increased adsorption of proteins and promoted actin stress fiber formation. Moreover, plasma technique was found to modify levels of chemical groups, such as $-\text{COOH}$, $-\text{OH}$, or $-\text{NH}_2$ on scaffold surfaces, and so influence the cell–substrate interactions. For example, human umbilical vein endothelial cell (HUVEC) adhesion was improved by plasma treatment of PLA through the control of carbon and oxygen concentration,¹⁹ and human embryonic palatal mesenchyme (HEPM) cell proliferation was increased by plasma-treated poly(ether ether ketone) (PEEK) through assembling amino groups on the surface.²⁰ Amino-rich PLA surfaces created by plasma treatment were also reported to promote osteogenic differentiation of MC3T3-E1 cells.¹⁷ These results support the feasibility of plasma technology to regulate the biological functions of biomaterials. However, the effects of plasma treatment on the surface of PLLA nanofibrous membranes, and the subsequent dose-dependent cellular response and osteogenesis of MSCs, are yet to be clarified.

Herein, the physicochemical properties and biological functions of PLLA nanofibers after low-temperature atmospheric plasma treatment over periods of 1, 5, or 10 min were explored. We have characterized the hydrophilicity and chemical changes on the surfaces of these nanofibers, as well as the ability of these nanofibers to promote the adhesion, proliferation, and differentiation of BMSCs.

Materials and methods

Preparation of electrospun PLLA nanofibers scaffold

PLLA powder (0.7 g) was added to 10 mL of trifluoroethanol (TFE) and stirred overnight to ensure the solution was completely dissolved. The PLLA/TFE solution was ejected using a 20-mL syringe with a steel needle (inner diameter of 0.5 mm) at a rate of 0.7 mL/h via a programmable syringe pump (Top 5300, Japan). A metal plate (20 cm × 25 cm) was placed 18 cm from the tip of the needle and used to collect the randomly arranged nanofibers. During ejection, a constant voltage (15 kV; DW-P303-1AC, Tianjin Dongwen High-voltage Power Supply Plant, China) was applied between the metal plate and the needle tip. Nanofibers were then incubated in a vacuum oven (DZF-6210; Bluepard Instruments Co., China) at room temperature for 2 weeks to remove residual solvent.

Plasma treatment of PLLA nanofibers

PLLA nanofibrous membranes were cut into disks (diameter 2.5 cm), placed into a low-temperature plasma cleaner (Harrick Plasma PDC32G, USA) and maintained at 18 W for periods of 1, 5, or 10 min. After treatment, samples were sealed in an airtight argon-filled chamber. The morphology of the nanofibers was observed by scanning electron microscopy (SEM), and the fiber diameter was measured from the SEM photographs using image analysis software (Image J; National Institutes of Health, USA).

Water contact angle measurement. To evaluate the hydrophilicity of the nanofibrous membranes, static water contact angles of each sample were measured at 25°C and 65% humidity using a Cam 200 Optical Contact Angle Meter (KSV Instruments, USA). Approximately 5 μ L of distilled water was dropped onto each sample, and images of the droplet were recorded after 5 s. The contact angles were calculated by computer analysis of the acquired images.

X-ray photoelectron spectroscopy. Surface chemical changes were determined by X-ray photoelectron spectroscopy (XPS; Thermo V6 Escalab 250; Thermo VG Scientific, UK) in a vacuum chamber with an anode voltage of 15 kV and a current of 10 mA. High-resolution spectra of regions of interest were recorded, at a pass energy of 20 eV.

Cell culture and seeding

Rat BMSCs were obtained from Cyagen Biosciences, Inc. (China). The culture medium contained rat MSC basal medium supplemented with 10% MSC-qualified fetal bovine serum (FBS), 100 IU/mL penicillin–streptomycin, and 2 mM glutamine (all from Cyagen Biosciences, Inc.). The medium was changed every 2–3 days. Once BMSCs reached 80–90% confluence, cells were detached with 0.25% trypsin/EDTA (Gibco, Life Technologies, USA) and subcultured at a density of 5×10^5 cells in a T75 flask. BMSCs were passaged three times before being used. Untreated or

plasma-treated PLLA nanofibrous membranes were placed into six-well plates and sterilized with ultraviolet (UV) light for 1 h. Cells were cultured on these membranes in media containing osteogenic additives, including 50 mg/mL ascorbic acid, 10 mM sodium β -glycerol phosphate, and 10^{-8} M dexamethasone. Control cells were cultured on TCPs without any osteogenic additives. All experiments were done in triplicate.

Cellular morphology observation

One day after cell seeding, the cellular morphology was observed by SEM (Top 5300) with an accelerating voltage of 15 kV. BMSCs were washed with phosphate-buffered saline (PBS) and fixed with 2.5% glutaraldehyde for 2 h and then treated with 0.18 M sucrose solution. The samples were rinsed three times with water, and then dehydrated through a series of graded alcohol solutions before being air-dried overnight. The scaffolds were coated with gold using a sputter coater (Jeol JFC-1200 Fine Coater; Jeol, Japan) before observation.

Cell proliferation

Cell proliferation was evaluated using a Cell Counting Kit (Dojindo, Japan), based on a water-soluble tetrazolium salt (WST-8). After cells were cultured on nanofibrous membranes for periods of 1, 3, 5, or 7 days, the WST-8 reagent was added and incubated for another 4 h protected from light. Then, 200 μ L of each sample was added to a 96-well plate, and the absorbance was measured at 450 nm using a microplate reader (Bio-Rad 680; Microplate Master, USA).

Real-time quantitative reverse transcription–polymerase chain reaction analysis. To assess the change in expression of various osteogenic-specific marker genes, real-time quantitative reverse transcription–polymerase chain reaction (qRT-PCR) on BMSCs cultured on untreated or plasma-treated nanofibers for selected times were performed. These genes included COL1A1, osteopontin (OPN), OCN, ALP, bone morphogenetic protein 2 (BMP2), and runx2 (RUNX2). The fold change in expression of these genes during differentiation was determined after 4 or 7 days of culture.

BMSCs were seeded at a concentration of 5.0×10^4 cells per wafer, and cultured for the indicated times. Total RNA was then extracted using RNeasy Mini Kit (Qiagen, Hilden, Germany), following the manufacturer's instructions. RNA (1 μ g) was added to a 20- μ L RT reaction mixture containing 10 \times RT buffer, 25 mM MgCl₂, 10 mM dNTPs, recombinant RNasin ribonuclease inhibitor, 15 U AMV (Avian Myeloblastosis Virus) Reverse Transcriptase (Promega, Madison, USA) and 0.5 μ g oligo (dT) primer. SYBR green-based RT-PCR was performed with an ABI PRISM 7500 RT-PCR System (Applied Biosystems, Life Technologies, USA) under the following conditions: 45 cycles of 95°C for 30 s, 60°C for 30 s, and 72°C for 30 s. Glyceraldehyde-3-phosphate dehydrogenase (GAPDH) was used as the housekeeping gene. Quantification of gene expression was based on the C_T value, which was calculated as the average of three replicate measurements for each sample analyzed. All primers were synthesized based on the sequences of the corresponding rat mRNAs (messenger RNAs) in GenBank. The primers used are as follows: RUNX2, 5'-TTC TGTCTGTGCCTTCTTG-3', 5'-AATGCCTCCGCTGTTATG-3'; BMP2, 5'-GCT TCCGCTGTTT GTGTTT-3', 5'-TAGTGACTTTTGGCCACGACG-3'; ALP, 5'-AGGGAAGGGTCAGTCAG GTT-3', 5'-TACTCGGACAATGAGATGC-3'; COL1A1, 5'-CCACCCAGGGATAAAA-3', 5'-GGAGAGAGTGCCAACTCCAG-3'; OPN, 5'-ATCGGACTCCTGGCTCTTC-3', 5'-GCTTGGCTTACG GAC TGAG-3'; and OCN, 5'-CTAGCTCGTCACAATTGGGGTT-3', 5'-ATGAGGACCC TCTCTCTGCTCA-3'.

ALP activity. ALP activity of BMSCs cultured for periods of 2, 4, and 7 days were measured using the ALP Assay Kit (Abcam, Cambridge, UK) according to the manufacturer's instructions. The kit had *p*-nitrophenyl phosphate (pNPP) as the phosphatase substrate as it turns yellow when dephosphorylated by ALP. Culture supernatants (30 μ L) were collected from each well. Samples were put in alkaline buffer, and added with 50 μ L pNPP solution. After incubating for 60 min, the reaction was stopped with 20 μ L stop solution: the absorbance at 405 nm was then measured. This experiment was based on standard curve which from Kit itself to quantify ALP activity. ALP activity of the test samples can then be calculated as follows:

$$\text{ALP activity (U/mL)} = \frac{\text{Amount of pNPP generated}}{\text{Volume of sample/Reaction time}}$$

Statistical analysis

All experimental results and measurements were performed in triplicate and expressed as the mean \pm standard deviation (SD). Statistical analysis was performed using the Student's paired *t*-test, and *p* values less than 0.05 were considered significant.

Results

Characterization of PLLA nanofibers

SEM was used to identify plasma treatment-induced changes on the PLLA nanofibers. As shown in Figure 1, untreated nanofibers were predominantly straight, while treated nanofibers exhibited slight curvature. We could identify crosslinking between nanofibers after plasma treatment as well as a decrease in the fiber diameter.

Plasma treatment increased the hydrophilicity of PLLA nanofibers

Images of water droplets on the various samples are shown in Figure 2. The water contact angle on untreated nanofibers was 115.3°. On treated nanofibers, the contact angle decreased inversely to the time of plasma treatment. Nanofibers treated for 1 min had a water contact angle of 96°, and it was significantly reduced to 53.8° after a 5-min treatment. After 10 min, we observed very pronounced surface hydrophilicity. Because of this, stable water droplets could not be maintained on the surface and infiltrated into the membranes immediately: therefore, no data from this group of samples are presented here.

Plasma treatment-induced chemical changes of PLLA nanofibers

XPS was performed to measure the surface chemical characteristics of nanofibers before and after plasma treatment. The results depicted in Figure 3 indicate that the nitrogen content in the surface of PLLA nanofibers was increased significantly after plasma treatment. The group treated for 10 min had the highest nitrogen content, followed by the groups treated for 5 and 1 min. This nitrogen content was considered to represent the existence of amino groups on the surface of plasma-treated PLLA nanofibers. It demonstrates that plasma treatment can increase amino content on the surface of PLLA nanofibers in a time-dependent manner.

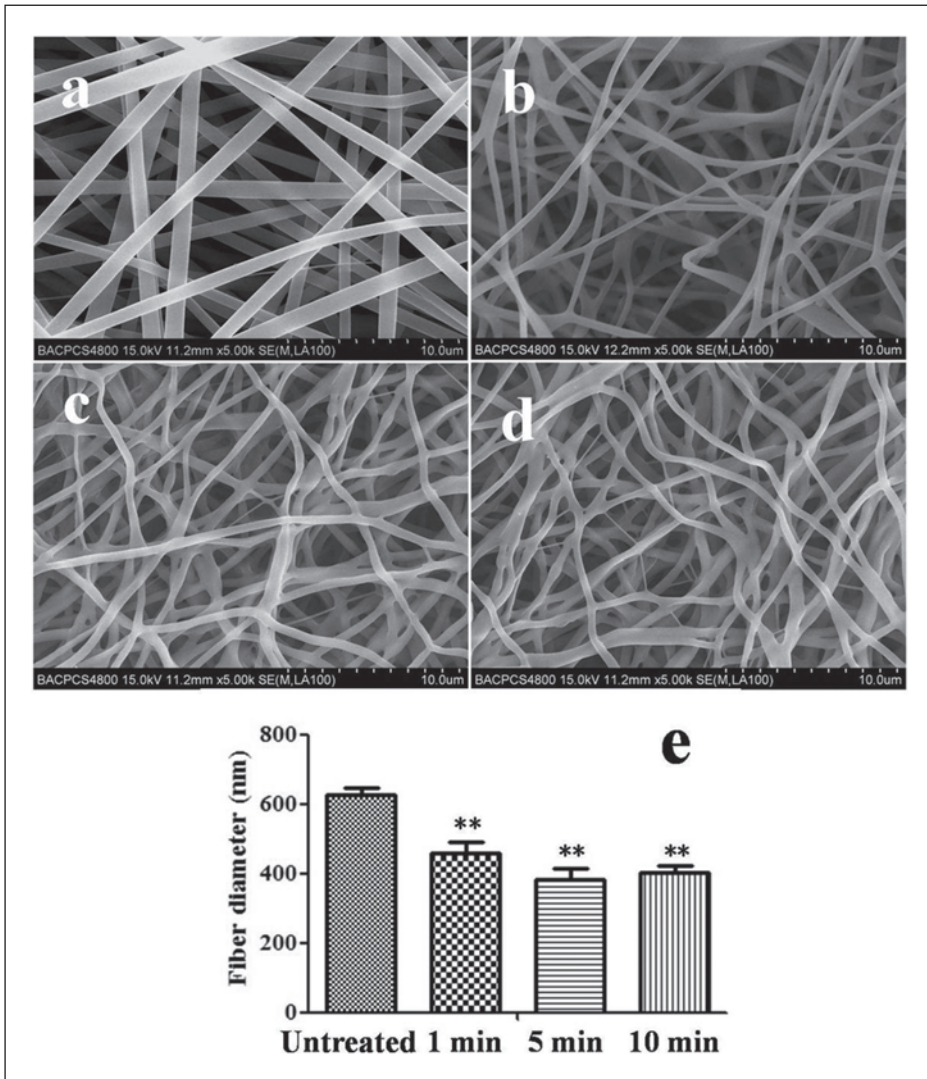


Figure 1. SEM images of (a) untreated PLLA nanofibers and plasma-treated for (b) 1, (c) 5, and (d) 10 min. (e) The fiber diameter (nm) of untreated and plasma-treated nanofibers ($n = 100$).

SEM: scanning electron microscopy; PLLA: poly(L-lactic acid).

* $p < 0.05$ and ** $p < 0.005$.

BMSCs morphology and proliferation

Rat BMSCs were used as model cells because of their well-documented osteogenic differentiation and their sensitive response to the culture environment. As shown in Figure 4, cells cultured on nanofibers treated for 1 min spread more than those cultured on untreated nanofibers. Cells cultured on the nanofibers treated for 5 min showed the greatest extent of spreading among all the groups. Unexpectedly, cells cultured on nanofibers treated for 10 min did not spread as well as those on the samples treated for 1 or 5 min. Quantitative measurements of the cell areas confirmed

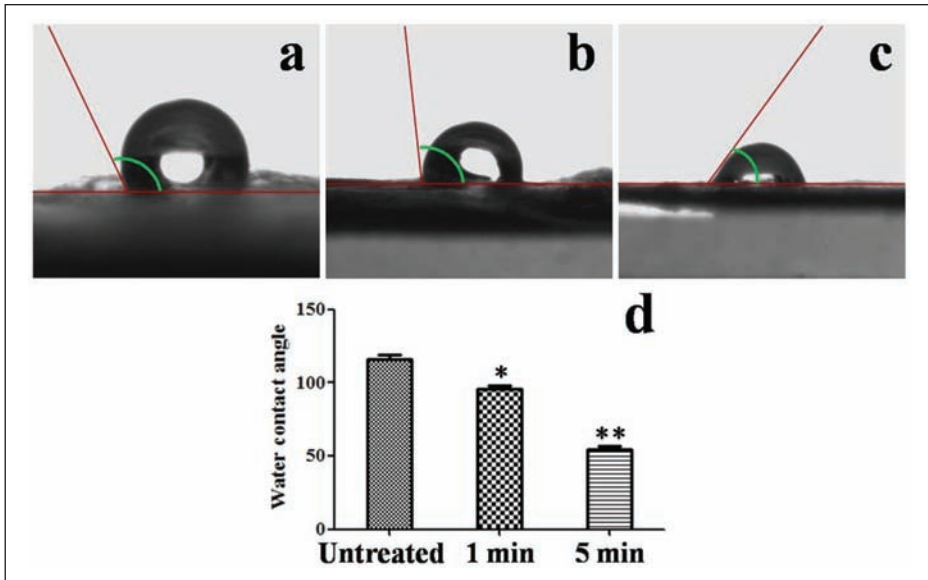


Figure 2. Typical water droplet images of distilled water 5 s after being dropped onto an (a) untreated or plasma-treated PLLA nanofibers surface for (b) 1 and (c) 5 min. (d) The water contact angle measured from the indicated samples ($n = 30$).

PLLA: poly(L-lactic acid).

It should be noted that water droplet did not stay on the surface of the 10-min group; hence this group is not represented here.

* $p < 0.05$ and ** $p < 0.005$.

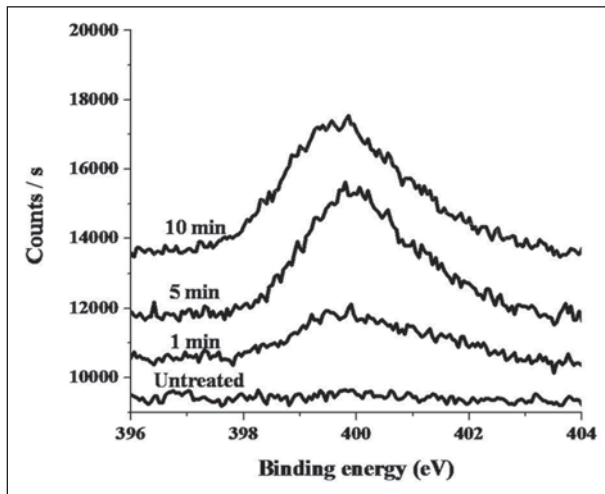


Figure 3. X-ray photoelectron spectroscopy (XPS) analysis of the nitrogen content of PLLA nanofibers before and after plasma treatment.

PLLA: poly(L-lactic acid).

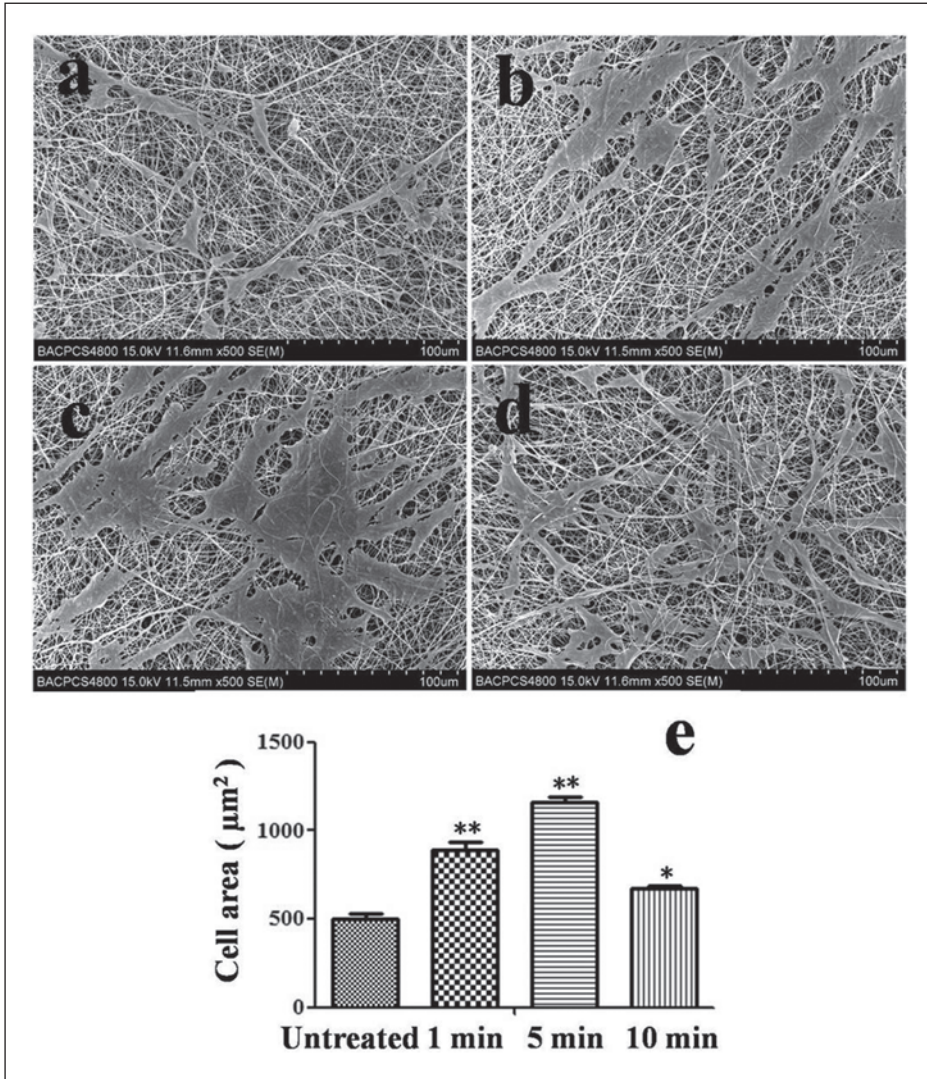


Figure 4. SEM images of BMSCs after 1 day of culture on (a) untreated or plasma-treated PLLA nanofibers for (b) 1, (c) 5, and (d) 10 min. (e) The cell spreading area measured from the indicated samples ($n = 20$).

SEM: scanning electron microscopy; BMSC: bone marrow stromal cell; PLLA: poly(L-lactic acid).

* $p < 0.05$ and ** $p < 0.005$.

our observations, where cell areas were greatest on samples treated for 5 min, followed by those treated for 1, 10 min, and finally, untreated samples.

Using a CCK-8 proliferation assay, as shown in Figure 5, we demonstrated that plasma treatments of 1 and 5 min significantly increased BMSC proliferation. However, cells cultured on nanofibers treated for 10 min had no increase in proliferation compared with those cultured on untreated nanofibers.

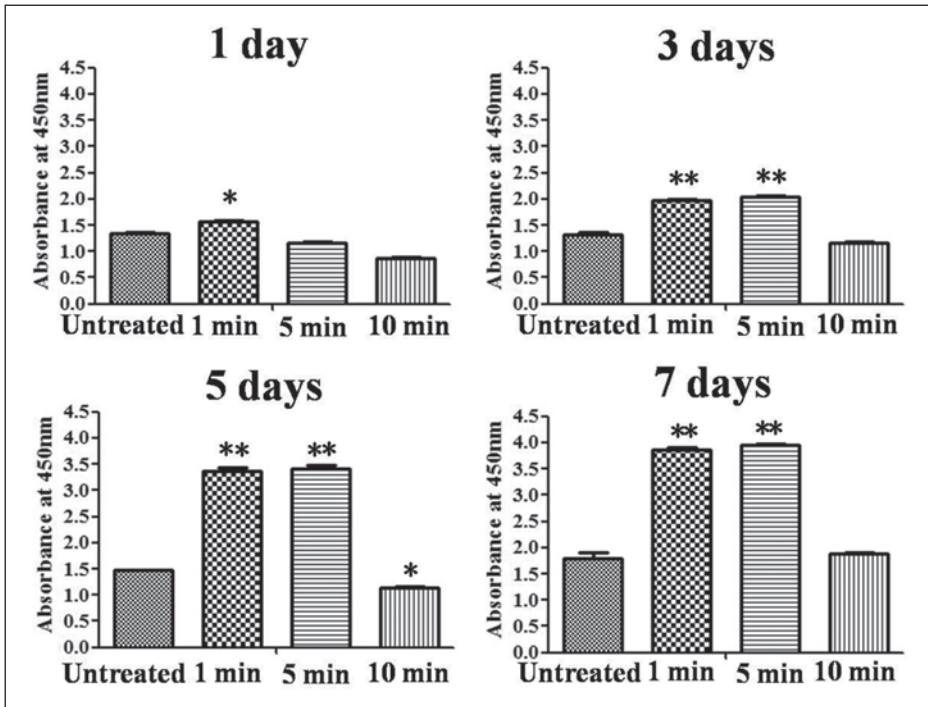


Figure 5. Cell proliferation analyzed by the absorbance measured at 450 nm for the indicated samples for 1, 3, 5, and 7 days.

* $p < 0.05$ and ** $p < 0.005$.

Expression profiles of osteogenic-specific genes

We analyzed the expression level of osteogenic-specific genes including RUNX2, BMP2, ALP, COL1A1, OPN, and OCN by qRT-PCR. As shown in Figure 6, RUNX2 was most highly expressed in BMSCs cultured on nanofibers treated for 5 min, with 5-fold (after 4 days) and 7-fold (7 days). Cells cultured on 10-min-treated samples showed less expression of RUNX2 than the 1-min-treated samples, but higher expression than those on the untreated nanofibers. BMP2 expression in BMSCs cultured on 5-min-treated nanofibers was increased to 2-fold and 4-fold after 4 and 7 days, respectively. Little difference in BMP2 expression was observed between the 1- and 10-min groups at 4 days, but its expression at 7 days in the 1-min group was much higher than the 10-min group. The expression of ALP, a marker of early osteogenic differentiation, reached up to 20-fold (4 days) and 32-fold (7 days) in the 5-min group. BMSCs cultured on the 1-min-treated nanofibers showed slightly higher ALP expression at 7 days (20-fold) than those on the untreated group, which was similar to the 10-min group (18-fold). The COL1A1, one of the major components of extracellular matrix and an early marker of osteogenic differentiation of BMSCs expression, was increased 16-fold in the 5-min group at 4 days and maintained a similar level (17-fold) at 7 days. At 4 days, COL1A1 expression was similar (12-fold) in BMSCs cultured on untreated, 1-, and 10-min groups. After 7 days, COL1A1 levels in the untreated and 10-min groups were similar to those in the 5-min group, but it was still relatively lower (14-fold) in the 1-min-treated samples. OPN is associated with cell proliferation and differentiation. The expression level of OPN at 4 days in untreated, 1-,

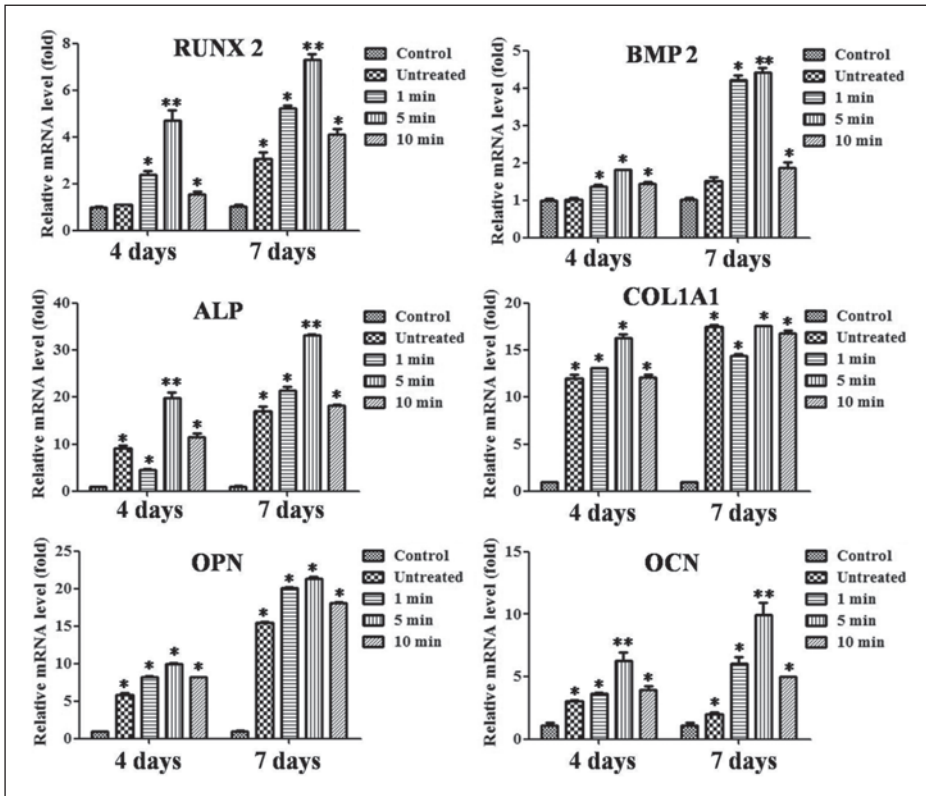


Figure 6. Cells cultured on untreated or plasma-treated PLLA nanofibers for 1, 5, and 10 minutes under osteogenic conditions.

qRT-PCR: quantitative reverse transcription–polymerase chain reaction; PLLA: poly(L-lactic acid).

Levels are shown as the fold-increase compared with control.

* $p < 0.05$ and ** $p < 0.005$.

5-, and 10-min groups showed a 6-, 8-, 10-, and 8-fold up-regulation, respectively. After 7 days, OPN was up-regulated by 15-, 20-, 22-, and 18-fold. OCN is regarded as a crucial protein for mature osteoblasts. OCN expression in the 5-min group showed the highest increases (6-fold for 4 days and 10-fold for 7 days). After 7 days, the expression in the 1-min group was increased 6-fold, while it only increased 2-fold in the untreated group. Together, we found that OPN, OCN, RUNX2, and BMP2 showed similar trends in their increase in expression levels, while COL1A1 and ALP were more distinct. As shown in Figure 7, 2.5% agarose gel electrophoresis was performed to confirm the products of PCR.

ALP activity

As shown in Figure 8, the 5-min group had the highest ALP activity, which reached up to 4, 9, and 14 mU/mL after 2, 4, and 7 days, respectively. ALP activity in the 1-min group showed slightly lower activities of 3, 7, and 11 mU/mL, while there was no significant difference between the 10-min and untreated groups.

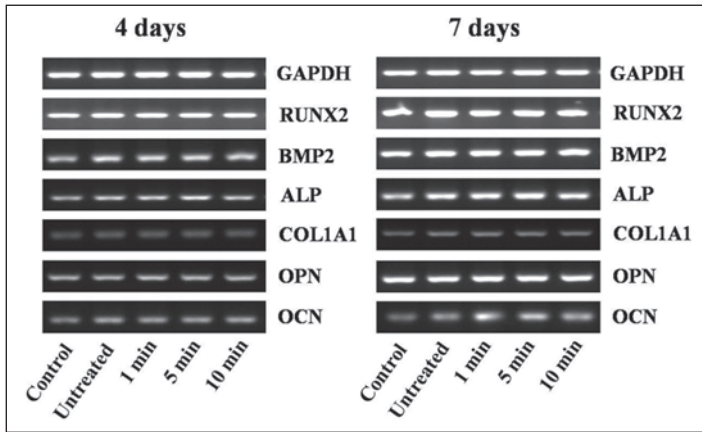


Figure 7. Images of the PCR products after electrophoresis through a 2.5% agarose gel. PCR: polymerase chain reaction; GAPDH: glyceraldehyde-3-phosphate dehydrogenase.

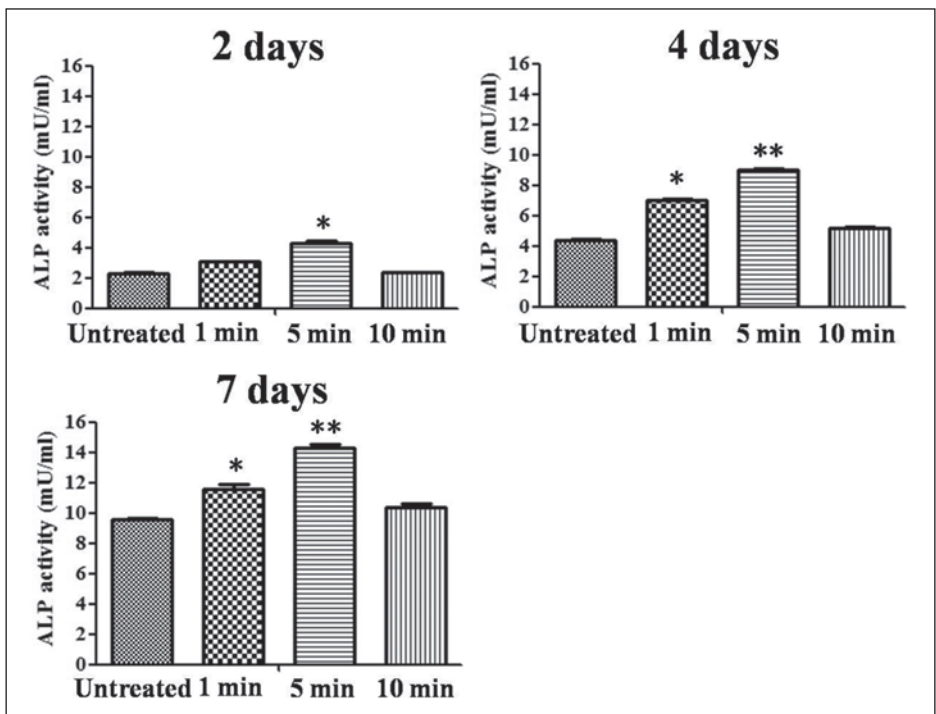


Figure 8. Quantification of ALP activity in culture supernatants of BMSCs after 2, 4, and 7 days cultured with osteogenic differentiation medium in the indicated groups.

BMSC: bone marrow stromal cell.

* $p < 0.05$ and ** $p < 0.005$.

Discussion

Surface energy is considered to be an important surface feature of biomaterials, affecting the cellular response. It is clear that hydrophilic surfaces promote better cell adhesion, spreading, and function compared to hydrophobic surfaces. Although electrospun PLLA nanofibers have been shown to be useful in tissue engineering and regenerative medicine,¹⁴ their hydrophobic properties and surface inertia might limit their biomedical applications.¹⁵ Low-temperature plasma treatment provides an effective method to modify the surface chemistry/energy of polymeric biomaterials,²¹ and many reports have indicated that these modifications can affect cellular functions.²²

It was found that a low-temperature atmosphere plasma improved the surface hydrophilicity of electrospun PLLA nanofibers, and subsequently, played time-dependent effects on rat BMSCs osteogenic differentiation. The amino content on the surface of PLLA nanofibers was increased by plasma treatment in a time-dependent manner, which then proportionately increased the hydrophilicity of the surface. The BMSCs cultured on plasma-treated nanofibers spread better with a larger cellular area and proliferated faster compared with those on untreated ones. Unexpectedly, however, these cellular responses were not proportional to treatment times. In all cases, BMSCs cultured on nanofibers treated for 5 min exhibited the greatest spreading extent and the fastest growth. qRT-PCR analysis further confirmed that 5-min treatment group led to the highest expression of selected osteogenic marker genes. We also found ALP activity to be highest in BMSCs cultured on nanofibers with 5-min plasma treatment.

Therefore, low-temperature plasma is an effective strategy for modifying the surface features of PLLA nanofibers, which results in significant enhancement in cellular functions. Atmospheric oxygen and nitrogen were ionized through an electric discharge process, and active molecules such as O₃, NO, and NO₂ were abundantly produced.²³ These active molecules interacted with the nanofiber surfaces and generated functional groups, which can affect surface properties such as wettability.¹⁷

It is widely held that the surface hydrophilicity of biomaterials is a property crucial to the governance of their biological activities.¹⁵ Protein adhesion plays a pivotal role in the regulation of subsequent cell behaviors,²⁴ and this process of adhesion can be effected by the hydrophilicity of the biomaterial surface.²⁵ D'Sa et al.¹⁸ reported that albumin binds to hydrophobic surfaces very strongly and irreversibly, preventing further attachment of other proteins, such as the extracellular matrix components, which are required for cell attachment. Andrade and Hlady²⁶ showed that cell adhesion and spreading involved a series of competitive protein adsorption events. They demonstrated that the adsorption of these proteins on the substrate was a prerequisite for cell adhesion, spreading, and proliferation. Hydrophilic surfaces contain a water layer and promotes reversible albumin adsorption, facilitates the attachment of proteins to the surface, and increases cell attachment and actin stress fiber formation.¹⁸

Although low-temperature plasma treatment of PLLA nanofibers increased cell spreading and proliferation and the 10-min treatment of nanofibers generated the highest hydrophilicity, however, the cells cultured on these nanofibers had reduced spreading and proliferation compared to the 5-min-treated nanofibers. It is possible that plasma treatment for 5 min may only modify the outer surface of nanofibrous membranes, leading to protein enrichment where the membrane contacts with the cells. Longer treatment times might also modify the inner part of the membranes, which is a likely explanation of the immediate disappearance of the water droplet in the contact angle assay. This could lead to an accumulation of adsorbed protein in the interior of the membranes, effectively reducing their exposure to the cells.

The expression level of osteogenic-specific genes including RUNX2, BMP2, ALP, COL1A1, OPN, and OCN, and the activity of ALP were closely related to the morphological phenotypic behavior of the cells. BMSCs in the 5-min group exhibited the highest expression of all the selected genes and the highest ALP activity at the early differentiation stages of 4 and 7 days. This indicated that the 5-min plasma treatment of PLLA was the most effective to promote osteogenic differentiation of BMSCs. Aspects of BMSC morphology such as size and shape are closely related to the extent of BMSC differentiation and lineage determination.^{27–29} Peng et al.³⁰ reported that small BMSCs were associated with adipogenic differentiation of MSCs and large sizes favored osteogenic differentiation. Kumar et al.¹³ illustrated that an elongated and highly branched shape is characteristic of osteogenic morphology, and this morphology could commit the BMSC differentiating into an osteogenic lineage. From 4 to 7 days, the expression level of all the selected genes in all the plasma treatment groups increased significantly, except for COL1A1, whose expression level was more static. This might be because COL1A1 is an early marker of BMSC differentiation, and its expression might be fully increased before 4 days in our system.

In addition to improved hydrophilicity, plasma treatment-induced chemical changes on the surfaces of PLLA nanofibers might also contribute to the enhanced behavior of rat BMSCs.^{31–36} Curran et al.²¹ reported that amino-rich surfaces could promote osteogenic differentiation of MSCs both in basic and osteogenic induction conditions, and chondrogenesis was promoted by –COOH and –OH groups. Barradas et al.¹⁷ also reported that amino assembled on the surface of biomaterials could improve osteogenesis of MC3T3-E1 cells. In short, the promotion of osteogenesis by amino-modified surfaces has been widely reported,^{37,38} and these were consistent with the enhanced osteogenic behavior of BMSCs in our study.

Conclusion

In conclusion, low-temperature atmosphere plasma treatment is an effective method to improve hydrophilicity of the electrospun PLLA nanofibers and to enrich amino groups on their surface. Optimization of plasma treatment time led to significant enhancement of cell behaviors, such as adhesion, proliferation, and osteogenic differentiation of BMSCs. Thus, low-temperature plasma treatment is a feasible technology for the improving the biocompatibility and osteogenic function of PLLA nanofibers, and is an exciting potential strategy for the surface modification of biomaterials.

Declaration of conflicting interests

The authors declare that there is no conflict of interest.

Funding

This study was supported by the National Basic Research Program of China (2012CB933900), National Natural Science Foundation of China (81171000), and the National High Technology Research and Development Program of China (2012AA022501).

References

1. Li S, Yan Y, Xiong Z, et al. Gradient hydrogel construct based on an improved cell assembling system. *J Bioact Compat Polym* 2009; 24: 84–99.
2. Engler AJ, Sen S, Sweeney HL, et al. Matrix elasticity directs stem cell lineage specification. *Cell* 2006; 126(4): 677–689.

3. Zhu H, Cao B, Zhen Z, et al. Controlled growth and differentiation of MSCs on grooved films assembled from monodisperse biological nanofibers with genetically tunable surface chemistries. *Biomaterials* 2011; 32(21): 4744–4752.
4. Ma X, Wang Y, Guo H, et al. Nano-hydroxyapatite/chitosan sponge-like biocomposite for repairing of rat calvarial critical-sized bone defect. *J Bioact Compat Polym* 2011; 26: 335–346.
5. Gamboa-Martínez TC, Gómez Ribelles JL and Gallego Ferrer G. Fibrin coating on poly(L-lactide) scaffolds for tissue engineering. *J Bioact Compat Polym* 2011; 26: 464–477.
6. Re'em T and Cohen S. Microenvironment design for stem cell fate determination. *Adv Biochem Eng Biot* 2012; 126: 227–262.
7. Hosseinkhani H, Hosseinkhani M and Kobayashi H. Design of tissue-engineered nanoscaffold through self-assembly of peptide amphiphile. *J Bioact Compat Polym* 2006; 21: 277–296.
8. Ma J, He X and Jabbari E. Osteogenic differentiation of marrow stromal cells on random and aligned electrospun poly(L-lactide) nanofibers. *Ann Biomed Eng* 2011; 39(1): 14–25.
9. Beskardes IG and Gümüşderelioglu M. Biomimetic apatite-coated PCL scaffolds: effect of surface nanotopography on cellular functions. *J Bioact Compat Pol* 2009; 24: 507–524.
10. Powell HM, Supp DM and Boyce ST. Influence of electrospun collagen on wound contraction of engineered skin substitutes. *Biomaterials* 2008; 29(7): 834–843.
11. Guarino V, Alvarez-Perez M, Cirillo V, et al. HMSC interaction with PCL and PCL/gelatin platforms: a comparative study on films and electrospun membranes. *J Bioact Compat Polym* 2011; 26: 144–160.
12. Ruckh TT, Kumar K, Kipper MJ, et al. Osteogenic differentiation of bone marrow stromal cells on poly(epsilon-caprolactone) nanofiber scaffolds. *Acta Biomater* 2010; 6(8): 2949–2959.
13. Kumar G, Tison CK, Chatterjee K, et al. The determination of stem cell fate by 3D scaffold structures through the control of cell shape. *Biomaterials* 2011; 32(35): 9188–9196.
14. Wang B, Cai Q, Zhang S, et al. The effect of poly(L-lactic acid) nanofiber orientation on osteogenic responses of human osteoblast-like MG63 cells. *J Mech Behav Biomed* 2011; 4(4): 600–609.
15. Wan Y, Tu C, Yang J, et al. Influences of ammonia plasma treatment on modifying depth and degradation of poly(L-lactide) scaffolds. *Biomaterials* 2006; 27(13): 2699–2704.
16. Wang H, Kwok DT, Xu M, et al. Tailoring of mesenchymal stem cells behavior on plasma-modified polytetrafluoroethylene. *Adv Mater* 2012; 24(25): 3315–3324.
17. Barradas AM, Lachmann K, Hlawacek G, et al. Surface modifications by gas plasma control osteogenic differentiation of MC3T3-E1 cells. *Acta Biomater* 2012; 8(8): 2969–2977.
18. D'Sa RA, Burke GA and Meenan BJ. Protein adhesion and cell response on atmospheric pressure dielectric barrier discharge-modified polymer surfaces. *Acta Biomater* 2010; 6(7): 2609–2620.
19. Shah A, Shah S, Mani G, et al. Endothelial cell behaviour on gas-plasma-treated PLA surfaces: the roles of surface chemistry and roughness. *J Tissue Eng Regen Med* 2011; 5(4): 301–312.
20. Briem D, Strametz S, Schroder K, et al. Response of primary fibroblasts and osteoblasts to plasma treated poly(ether ether ketone) (PEEK) surfaces. *J Mater Sci: Mater Med* 2005; 16(7): 671–677.
21. Curran JM, Chen R and Hunt JA. The guidance of human mesenchymal stem cell differentiation in vitro by controlled modifications to the cell substrate. *Biomaterials* 2006; 27(27): 4783–4793.
22. Pavlica S, Piscioneri A, Peinemann F, et al. Rat embryonic liver cell expansion and differentiation on NH₃ plasma-grafted PEEK-WC-PU membranes. *Biomaterials* 2009; 30(33): 6514–6521.
23. Dong KY, Ham DJ, Kang BH, et al. Effect of plasma treatment on the gas sensor with single-walled carbon nanotube paste. *Talanta* 2012; 89: 33–37.
24. Chen WL, Lin CT, Lo HF, et al. The role of protein tyrosine phosphorylation in the cell–cell interactions, junctional permeability and cell cycle control in post-confluent bovine corneal endothelial cells. *Exp Eye Res* 2007; 85(2): 259–269.
25. Cole MA, Voelcker NH, Thissen H, et al. Stimuli-responsive interfaces and systems for the control of protein-surface and cell-surface interactions. *Biomaterials* 2009; 30(9): 1827–1850.
26. Andrade JD and Hlady V. Vroman effects, techniques, and philosophies. *J Biomater Sci: Polym Edn* 1991; 2(3): 161–172.
27. Folkman J and Moscona A. Role of cell shape in growth control. *Nature* 1978; 273(5661): 345–349.
28. McBeath R, Pirone DM, Nelson CM, et al. Cell shape, cytoskeletal tension, and RhoA regulate stem cell lineage commitment. *Dev Cell* 2004; 6(4): 483–495.
29. Tseng PC, Young TH, Wang TM, et al. Spontaneous osteogenesis of MSCs cultured on 3D microcarriers through alteration of cytoskeletal tension. *Biomaterials* 2012; 33(2): 556–564.
30. Peng R, Yao X, Cao B, et al. The effect of culture conditions on the adipogenic and osteogenic inductions of mesenchymal stem cells on micropatterned surfaces. *Biomaterials* 2012; 33(26): 6008–6019.
31. Woodfield TB, Miot S, Martin I, et al. The regulation of expanded human nasal chondrocyte re-differentiation capacity by substrate composition and gas plasma

- surface modification. *Biomaterials* 2006; 27(7): 1043–1053.
32. Mwale F, Wang HT, Nelea V, et al. The effect of glow discharge plasma surface modification of polymers on the osteogenic differentiation of committed human mesenchymal stem cells. *Biomaterials* 2006; 27(10): 2258–2264.
33. Chim H, Ong JL, Schantz JT, et al. Efficacy of glow discharge gas plasma treatment as a surface modification process for three-dimensional poly (D,L-lactide) scaffolds. *J Biomed Mater Res A* 2003; 65(3): 327–335.
34. Byun Y, Ko KB, Cho M, et al. Effect of hydrogen generated by dielectric barrier discharge of NH₃ on selective non-catalytic reduction process. *Chemosphere* 2009; 75(6): 815–818.
35. Faeda RS, Tavares HS, Sartori R, et al. Biological performance of chemical hydroxyapatite coating associated with implant surface modification by laser beam: biomechanical study in rabbit tibias. *J Oral Maxil Surg* 2009; 67(8): 1706–1715.
36. Tamargo-Martinez K, Martinez-Alonso A, Villar-Rodil S, et al. Surface modification of high-performance polymeric fibers by an oxygen plasma: a comparative study of poly(p-phenylene terephthalamide) and poly(p-phenylene benzobisoxazole). *J Chromatogr A* 2011; 1218(24): 3781–3790.
37. Keselowsky BG, Collard DM and Garcia AJ. Surface chemistry modulates focal adhesion composition and signaling through changes in integrin binding. *Biomaterials* 2004; 25(28): 5947–5954.
38. Keselowsky BG, Collard DM and Garcia AJ. Integrin binding specificity regulates biomaterial surface chemistry effects on cell differentiation. *Proc Natl Acad Sci USA* 2005; 102(17): 5953–5957.